NATIONAL ADVISORY COMMITTEE
FOR AERONAUTICS

TECHNICAL MEMORANDUM 1247

LANDING PROCEDURE IN MODEL DITCHING TESTS OF Bf 109

By W. Sottorf

Translation of "Der Landevorgang im Modellversuch.
Wasserlandung Bf 109." Institut für Seeflugwesen der Deutschen
Versuchsanstalt für Luftfahrt, E.V.

Washington

December 1949

NATIONAL ADVISORY COMMITTEE FOR AERONAUTICS

TECHNICAL MEMORANDUM 1247

LANDING PROCEDURE IN MODEL DITCHING TESTS OF Bf 109[*]

By W. Sottorf

Abstract: The purpose of the model tests is to clarify the motions in the alighting on water of a land plane. After discussion of the model laws, the test method and test procedure are described. The deceleration—time—diagrams of the landing of a model of the Bf 109 show a high deceleration peak of $> 20g$ which can be lowered to 4 to 6g by radiator cowling and brake skid.

I. PURPOSE OF THE TESTS

The carrier plane is a land plane used over water; thus the possibility of an emergency landing on water must be taken into consideration.

---

[*]"Der Landevorgang im Modellversuch. Wasserlandung Bf 109." Institut für Seeflugwesen der Deutschen Versuchsanstalt für Luftfahrt, E. V.

Landings on water were carried out without considerable damage with land planes, the landing speed of which lay, influenced by wind, below about 70 km/hrs[1]. However, with increasing landing speed the inclination for nosing-over in a normal landing, particularly for non-retractable landing gear, increases so greatly[2] that it is better — in order to avoid unnecessary losses in material and human lives — to use the model test for examination of the behavior of fast airplanes in a landing on water. With the aid of the model test the course of landings is shown for various operating conditions and the effect of appendices, as for instance landing gear and radiator, can be studied. As far as there is a possibility of improving unsatisfactory landing properties by auxiliary installations, the latter can be developed in the model test.

II. MODEL LAWS

With the entrance of a moving airplane into the free water surface external water forces appear which determine its motion. An essential part of the energy transmitted to the water by the airplane radiates out in the forming wave system which is under the influence of gravity. Aside from the forces of inertia (caused by the water mass in simultaneous motion and splashes) and the friction forces, forces of gravity also are in effect during the landing.

Perfect dynamic similitude which requires, for action of these three kinds of forces, not only observance of Newton's general law of similarity, but also of Froude's and Reynold's model law, is not attainable in the model test. Since, however, the forces of gravity in penetrating the water surface predominate compared with the friction forces, it is sufficient that the conditions of Froude's model law are satisfied, that is, that Froude's number is constant for model and full scale design:

$$F = \frac{v_H}{\sqrt{g l_H}} = \frac{v_M}{\sqrt{g l_M}} = \text{Const} \qquad \text{(Symbols p. 17)}$$

---

[1]Ar 66, Me 63
[2]Model W 34

If $\lambda = l_H/l_M$ is the model scale, the landing speed to be imparted to the model in order to initiate a landing of dynamically similar course is

$$v_{L_M} = \frac{v_{L_H}}{\sqrt{\lambda}}$$

Neglecting the influence of Reynold's law on air drag and profile properties[3], lift and drag of the model are, according to Newton's general similarity law, similar to the lift and drag of the full scale airplane in air, if the design of the model is outwardly geometrically similar and if model flying weight $G_M = \dfrac{G_H}{\lambda^3}$ and position of the center of gravity are similar.

Full scale design:

$$A = c_a F\rho/2v_H{}^2$$

$$W = c_w F\rho/2v_H{}^2$$

Model:

$$\frac{A}{\lambda^3} = c_a \frac{F}{\lambda^2} \rho/2\left(\frac{v_H}{\sqrt{\lambda}}\right)^2$$

$$\frac{W}{\lambda^3} = c_w \frac{F}{\lambda^2} \rho/2\left(\frac{v_H}{\sqrt{\lambda}}\right)^2$$

The gliding angle is the same for model and full scale design:

$$\tan \gamma = \frac{W}{A}$$

For translatory motion all similarity requirements are therewith fulfilled.

$$b_M = b_H$$

---

[3]Schlichting: Einfluss der Turbulenz und der Reynolds'schen Zahl auf die Tragflügeleigenschaften. (Influence of the turbulence and the Reynolds number on the wing properties.) Ringbuch der Luftfahrttechnik IA1.

For rotary motion

$$I_M = \frac{I_H}{\lambda^5}$$

is to be met as a further similarity condition; it is sufficiently
satisfied by

$$I_{y_M} = \frac{I_{y_H}}{\lambda^5}$$

since in a normal landing no other rotations occur but those about
the transverse axis.

Furthermore, the following relations are valid:

$$\omega_M = \omega_H \sqrt{\lambda}, \quad n_M = n_H \sqrt{\lambda}$$

$$\epsilon_M = \epsilon_H \lambda$$

In the construction of light models a complete similitude with
respect to the moment of inertia has not been attained as yet.

Thus the following correction is made for the transfer of
velocities and accelerations of rotation and corresponding fre-
quencies from the model·to the full scale airplane. If

$$I_M' = \kappa I_M$$

is the moment of inertia of the model which does not fully satisfy
the requirement of similitude, one has for the statement of the
dynamic fundamental equation of the rotary motion, under the effect

of a prescribed torque $M_M = \frac{M_H}{\lambda^4}$ for free oscillation[4]

---

[4]For oscillation at the water surface the correction is not
given because of the unknown mass of water in simultaneous oscil-
lation. However, it must lie between 1 and K since the oscil-
lating mass of water remains constant as the moment of inertia of the
mass varies.

$$M_M = I_M' \frac{d\omega'_M}{dt}$$

whereas for similar moment of inertia one would have

$$M_M = I_M \frac{d\omega_M}{dt}$$

Thus there is

$$I_M \frac{d\omega_M}{dt} = I_M' \frac{d\omega'_M}{dt} = \kappa I_M \frac{d\omega'_M}{dt}$$

and hence

$$\epsilon_M = \kappa \epsilon'_M$$

$$\omega_M = \kappa \omega'_M \quad \text{respectively.}$$

If the motion is recorded by movies one can, by varying the film-operating speed accordingly, make the angular velocity of the model ω_M and the advance coefficient $f_M = \frac{v_M}{l_M}$ (that is the coefficient indicating how many times its own length the model travels per second) equal to those of the full scale airplane; thus one obtains the impression of a direct observation of the full scale airplane (from an adequate distance).

If the model performs an oscillation with the frequency n_M, showing a speed of advance of v_M or, respectively, an advance coefficient $f_M = \frac{v_M}{l_M}$, the corresponding frequency of the full scale model is

$$n_H = \frac{n_M}{\sqrt{\lambda}}$$

for a speed of advance

$$v_H = v_M \sqrt{\lambda}$$

and an advance coefficient

$$f_H = \frac{v_H}{l_H} = \frac{v_M \sqrt{\lambda}}{l_M \lambda} = \frac{v_M}{l_M \sqrt{\lambda}}$$

If the film operating speed is reduced at the ratio $1/\sqrt{\lambda}$ the model frequency n_M is varied to

$$\frac{n_M}{\sqrt{\lambda}} = n_H$$

and the advance coefficient f_M changes to

$$\frac{f_M}{\sqrt{\lambda}} = \frac{v_M}{l_M \sqrt{\lambda}} = f_H$$

as intended.

For the presentation of the film a film speed of 16 frames per second is the lower limit if non-flickering pictures are to be obtained. The photographs are therefore taken appropriately with the film speed $> 16 \sqrt{\lambda}$ frames per second.

If one wants the frequency to equal that of the full scale airplane (taking the dissimilarity of the moment of inertia of the model into consideration) which is desirable for judging an oscillation phenomenon, the film operating speed must be reduced at the ratio $\kappa/\sqrt{\lambda}$ whence the advance coefficient becomes $f_H \kappa$; thus the speed appears to be κ times too high.

Rigidity of the Model

Investigations of dynamically similar airplane models[5] of customary design have shown that the rigidity of the model considerably exceeds that of the full scale model, so that the junctions must be weakened if similarity of the elastic properties is considered important.

For the present tests the comparatively greater strength of the model is very desirable because it makes a greater number of landings possible without having the model destroyed. However, one must take into consideration that a landing of the full scale model takes a dissimilar course, due to the appearance of additional or differently directed forces, from the moment when fuselage or wings break or considerable deformations occur.

III. TEST METHOD

. The model carried by the test carriage according to figure 1 is brought by the latter to the prescribed landing speed and then released from the guiding device. It glides into a covered space which is closed behind the model in order to prevent the model's being affected by the air motions caused by the test carriage, and lands on the water.

1. Air Flow Measurements at the Location of the Model

The model in starting is to be led through undisturbed air, influenced as little as possible by the test carriage. The only suitable location is in front, underneath the carriage. When the water level is lowered to a depth of water of 0.5 m, a free air cross section of 5 m width and 2 m height is at disposal.

At 1.75 m and 2.75 m distance ahead of the carriage the component of the relative air velocity $\left(v_{rel}\right)$ in the direction of travel and the deviation of v_{rel} compared with the horizontal was measured

---

[5]Michael: Herstellung dynamisch ähnlicher Flugzeugmodelle für Windkanalversuche zur Ermittlung der kritischen Geschwindigkeit. (Construction of dynamically similar airplane models for wind tunnel tests for determination of the critical velocity.) FB 51.

with respect to height. For the measurement of velocity Bruhn —
Venturi tubes were used, the reading of which is still satisfactory
for velocities of measurement of 8 to 14 m/s if, by check calibration
in the wind tunnel, the coefficient is determined as function of the
velocity. The direction was determined by means of a well—balanced
wind vane (fig. 5).

In figure 6 the horizontal component of the relative velocity
of the air (v_{tot}) is in proportion to the velocity of the
carriage (v_W), thus v_{tot}/v_W and the deviation from the
horizontal (γ^X) are plotted for the vertical section at the tank
center.

When a model is guided over the water surface at a height of 0.5 m
the carriage has the following effect on the air flow:

distance	1.75 m	2.75 m
v_{tot}/v_W	1.05	0.985
deviation γ^X	4° downward	4° downward

If, for instance, the wing lies in the range of the frontal and
the tail unit in the range of the rear cross section, the velocity
increases from the front toward the rear; a reduced velocity of
1.5 percent is transformed into an excessive velocity of 5 percent,
the oncoming flow deviating by 4° from the horizontal downward.

Thus the model is subjected to a flow during the uniform starting
flight; the force S which is equal in magnitude and opposite in
direction to the drag attacks, according to figure 7a, at the
horizontally guided center of gravity under an angle $\alpha_R = \alpha_g - \gamma^X$.
If this ground effect of the model were not taken into consideration,
the oncoming flow would strike the model, according to figure 7b,
under the larger angle $\alpha_R = \alpha_g + \gamma$. The free stream direction
changes, therefore, during the landing by the amount $\gamma + \gamma^X$. Since
thereby the moments are no longer compensated as they were during
the start, the airplane diminishes its angle of attack in approaching
the water surface if its static stability is sufficient.

The closeness of the ground affects the incidence in the same
manner.

2. Test Arrangement[6]

Figure 1 shows the test arrangement. The model is balanced with respect to an axis going through its center of gravity and is held at this axis by a fork-shaped cleat located at the end of the guide arm (fig. 2). The release of the model takes place, for a prescribed position of the test carriage, by means of a solenoid actuated by rail contact which releases the stopping device of the fork closed under spring pressure. The model now performs a gliding flight, entering by a gate the covered space at the tank end after a flight distance of about 6 m (fig. 3). The gate is closed immediately after the model has passed by an automatic closing device released by an observer, so that the landing occurs in an air space uninfluenced by the test carriage.

The automatic speed reduction for the test carriage starts after release of the model. The carriage passes the front part of the covered space. Thus it is necessary to swing up the guide arm by means of a hoisting apparatus (fig. 4) so that it comes to lie above the covering in a slot provided for that purpose. The operation of the hoisting device also takes place by means of a solenoid which begins to function shortly after release of the first solenoid. In the range of the guide arm the wooden covering is replaced by a ripping panel made of fabric in order to avoid destruction of the measuring apparatus in case of a failing of the solenoids.

3. The Model of the Bf 109 of Similar Mass[7]

The model of the Bf 109 selected for the first landing tests (fig. 9) was built according to the design developed by Dr. Krüger of the Institute for Aerodynamics in the plant North of the DVL. Its measurements are:

model scale $\lambda = 8$

span   b = 1.234 m

flying weight   G = 3.71 kg, corresponding to 1900 kg of the full scale airplane

---

[6]Design G. Schwarz, IfS.

[7]Design F. Lange, IfS.

position of the center of gravity   (cf. fig. 8)

moment of inertia $I_{yH} = 0.021 \text{ mkgs}^2 = 1.40 \dfrac{I_{yH}}{\lambda^5}$;

$$I_{yH} = 475 \text{ mkgs}^2$$

that is, the similar moment of inertia is exceeded by 40 percent.

IV. TEST PROCEDURE

1. Determination of the Landing Speed

Before performing a landing test one must determine the landing speeds of the model on the basis of the elevator deflection, the landing-flap deflection, and the aileron deflections considered. The lowest landing speed of the Bf 109 is about 120 km/hr.

Figure 10 gives a scheme of the test apparatus. The guide rod of the weight P attached at the centroidal axis is free to move in vertical direction and connected with the resistance dynamometer of the carriage by a cable line. At rest the cable line is G + P. By flights in the range of the landing speed the remaining weight (G + P) − A is determined and the corresponding angle of attack α_R of the fuselage axis is measured. One obtains by interpolation the landing speed v_L and the angle of attack α_R corresponding to the flying weight G (fig. 11).

The results are plotted in figure 12; in the upper part the elevator deflection β_H as $f(\alpha_R)$ for flap deflection $\beta_{K1} = 0$ to 40° and aileron deflection $\beta_Q = 20°$; in the lower part v_L as $f(\alpha_R)$ with β_{K1} and β_Q, respectively, as parameters. There results a model landing speed of 11.9 m/s, corresponding to 121 km/hr. for the full scale airplane.

2. Landing Test

For the landing, which is to take place at a prescribed landing speed, flaps and elevator were rigidly adjusted with the deflections resulting from figure 12. The tests carried out so far showed, however, that with the model approaching the water surface the incidence decreases (as detailed in III,1) so that pure tail landings could not be executed. In future tests the elevator will, therefore, be actuated by means of a small spring mechanism which starts working

at the moment the model is released, in order to counteract the rotation of the model.

The first tests were limited to observation and film recordings[8] of the phenomena. The landing distance was estimated and hence a mean deceleration determined.

After these tests had shown that the model easily withstood the stresses in landing an arrangement was made to fix the course of the landing for further tests. Since space limitations do not permit a sidewise film recording of the landing procedure, a mirror wall of 9 m length was erected laterally according to figure 1. The separate narrow mirrors standing vertically and spaced 0.4 to 0.8 m apart are arranged so that a beam normal to the flight direction impinging on them is reflected in the direction of the film camera located at the end of the landing space. The film is recorded at a speed of about 60 frames/sec; it is determined more accurately with the aid of the simultaneously photographed time signal. Points determining the position of the model in space – for instance wing, front part of the fuselage, tail unit and additional signs (fig. 13) – appear on the single photograph in sufficient number to set up a reliable s–t–diagram of the landing from which the v–t– and the b–t–diagram is determined by graphic differentiation. From the latter, one obtains by transformation the W–s–diagram. The differentiation is controlled by means of the energy equation, according to which, neglecting the vertical velocity,

$$\frac{1}{2} \frac{G}{g} v_E^2 = \frac{G}{g} \int_{s_1}^{s_2} C ds$$

if the immersion into the water takes place at s_1, the stopping at s_2 (Example fig. 19a).

V. RESULTS OF THE TESTS WITH THE BF 109

1. Tests from October 22 to 23, 1937

Film: Landing on the water of land planes, part 1.

---

[8]Film recordings; W. Fangerow, IfS jointly with the office for photography of the E – Office.

Preliminary tests:

a. The functioning of the entire test arrangement was examined with a trial model of simplified design (fig. 14).

b. Since it was possible that the model would be destroyed in its first landing on the water, a landing was first made on an oscillating landing strip in order to determine the landing point so as to be able to focus the film cameras on this point.

Landing test I:

Model without landing gear and tail wheel,
landing speed $v_L = 11.8$ m/s corresponding to 120 km/hr
slat extended, $\beta_{K1} = 40°$, $\beta_Q = 15°$, $\beta_H = -9°$, $\alpha_R = 14°$

Result:

Braking distance, estimated $< 1l$

mean deceleration ~ 6.1 g for model and full scale
                                   airplane

maximum elevation of the tail $\sim 75°$ with respect to horizontal

mean angular velocity $\omega_M = 7.85/s$ corresponding to

                                   $\omega_H = 2.77/s$

moment of inertia of the model, too large by 40 percent, taken into consideration, under neglect of the water mass in simultaneous oscillation:

$$\omega_{H_K} = 3.88/s$$

Landing test II

Repetition of test I.
Due to slight damage to a flap hinge the model dropped somewhat.

Landing test III

Model without landing gear and tail wheel
landing speed v_L = 12.8 m/s   corresponding to 130 km/hr
slat extended, β_{Kl} = 40°, β_Q = 15°, β_H = −3.5°, α_R = 8.5°

Result:

Braking distance, estimated $\sim$ 1.65l

mean deceleration $\sim$ 4.75 g for model and full scale
                                              airplane

(The calculation of the deceleration yields a lower result than in
test I because of the relatively rough estimate of the braking
distance).

Landing test IV.

Model with landing gear and tail wheel
landing speed v_L = 11.8 m/s   corresponding to 120 km/hr
slat extended, β_{Kl} = 40°, β_Q = 15°, β_H = −9°, α_R = 14°

Result:

Nose—over;

mean angular velocity in nosing over:

$$\omega_M = .85/s \text{ corresponding to } \omega_H = 3.13/s$$
$$\omega_{H_K} = 4.38/s$$

Summary 1.

The landing with landing gear leads to an immediate nose—over
whereas the landing without landing gear for a braking distance of
less than 1 fuselage length gives a mean deceleration of about 6 g.
The main reason for the strong braking effect is the radiator which
is struck frontally at the moment of immersion and thereby causes
a large drag.

By two means one attemps to obtain an improvement of the properties for a landing without landing gear:

1) Oblique covering of the radiator by a part of the fuselage fairing to be extended before the emergency landing.

2) Application of a ploughshare—like braking surface at the tail; its penetration into the water before the immersion of the fuselage should produce at the tail a braking force and a tailheavy downward force, thus obtaining a later immersion of the front part of the fuselage and radiator, and hence a lengthening of the braking distance.

2. Tests of December 22, 1937

Film: Landing on water of land planes, continuation.

Landing test V.

Landing with the radiator taken off, figure 15.
Model without landing gear and tail wheel
Landing speed $v_L = 11.8$ m/s corresponding to 120 km/hr
slat extended, $\beta_{Kl} = 40^\circ$, $\beta_Q = 15^\circ$, $\beta_H = -9^\circ$, $\alpha_R = 14^\circ$

In figure 19 there is plotted as a function of time the path curve determined from the film; the measured values are indicated. Furthermore the variation of the velocity and deceleration determined obtained by differentiation and the maximum elevation of the tail are given. In the film one can see — with particular clearness in the slow—motion part — that the flaps touch first; a deceleration up to about 1.5 g occurs which goes back to almost zero since the airplane pulls up again. At the second immersion the wing root rapidly penetrates and the maximum deceleration reaches 22.6 g, the tail simultaneously being elevated to about 80°, that is, the airplane comes close to nosing—over. The deceleration peak lies at the end of the braking distance at 0.4 v. During a time of 0.065 seconds the value of —6 g is exceeded; for the full scale airplane the corresponding time would be 0.185 seconds for equal deceler-ation (b = b_H). Figure 19a shows a control of the differentiation by means of the energy equation. (See p. 11.)

Landing test VI.

The radiator is provided with a cowling according to figures 16
and 18; otherwise like landing test V.
Variation of velocity and deceleration cannot be given because the
model lands outside of the row of mirrors.

Landing test VII.

Repetition of landing test VI.
The model lands again outside of the row of mirrors.

Landing test VIII.

Second repetition of landing test VI.
The release of the model from the holding device takes place 0.5
seconds earlier.
(Fig. 20). The model executes after the first immersion ($-b_{max}$ = 2 g),
due to the hydrodynamic lift caused by the fairing, a longer jump,
penetrates again with 0.7 v, $-b_{max}$ becoming 7.2 g for a maximum tail
elevation of about 30°; -6 g is exceeded during 0.05 seconds,
corresponding to 0.14 seconds for the full scale airplane.

Landing test IX.

Repetition of test VIII with increased landing speed.
landing speed v_{L} = 12.8 m/s   corresponding to 130 km/hr
slat extended, β_{Kl} = 40°, β_{Q} = 15°, β_{H} = -3.5^{o}, α_{R} = 8.5^{o}
(Fig. 21). The course of the landing is similar to the landing VIII.
The first deceleration maximum is 3 g, the second 8.9 g, for an
elevation of the tail of about 40°; -6 g is exceeded during 0.08
seconds, corresponding to 0.225 seconds for the full scale airplane.

Landing test X.

Model without landing gear and tail wheel with open radiator and
short brake-hook according to drawing, figure 18, and photograph,
figure 17.
Landing speed v_{L} = 11.8 m/s   corresponding to 120 km/hr
slat extended, β_{Kl} = 40°, β_{Q} = 15°, β_{H} = -9°, α_{R} = 14°
(Fig. 22). The immersion of the brake hook causes a gradually
increasing deceleration in the landing. For the immersion of the
fuselage the increase of the deceleration is no longer excessively

large. The maximum deceleration is 6.1 g, with a tail elevation
of about $60°$.

Landing test XI.

In order to speed up the effect of the brake hook, the brake
hook is lengthened (fig. 18); otherwise like landing test X (fig. 23).
The immersion of the hook causes a strong braking effect, $-b_{max} = 3.5 g$;
during the rotation about the transverse axis which is then initiated
the hook emerges from the water. The second immersion of the fuselage
occurs at 0.75 v; the slowly growing deceleration increases to 4.1 g
for a tail elevation of about $45°$.

Landing test XII.

Model without landing gear and tail wheel with open radiator and
lengthened brake hook, braking surface enlarged (fig. 18).
Landing speed $v_L = 12.1$ m/s   corresponding to 123 km/hr,
             otherwise like landing test X.
(Fig. 24) The enlarged surface of the hook probably does not grip
the water as well as the original surface (first case), the braking
for the first case is weaker; the immersion of the fuselage is less
favorable, which makes $-b_{max}$ increase to 8.1 g with increasingly
growing deceleration toward the end of the landing, for a tail
elevation of $50°$; -6 g is exceeded during 0.1 second, corresponding
to 0.28 s of the full scale model.

Summary 2.

By installation of a radiator cowling and application of a brake
skid the peaks of deceleration which exceed 20 g are lowered to 4
to 6 g.

The result of landing test XI with lengthened brake hook even
surpasses that of landing test VIII with cowled radiator. However,
if only one of the two means for improvement of the landing are to be
applied, the cowling of the radiator is more reliable since for
landings in the swell one can not count with certainty on an immersion
of the hook before the radiator penetrates the water surface, whereas
the favorable influence of a radiator cowling must always become
evident if the latter is not immediately deformed by the occurring
impact.

VI. SYMBOLS

Model		Index M
Full scale model		" H
F		Froude's number
f	1/s	advance coefficient
R		Reynolds' number
v_{tot}	m/s	horizontal component of v_{rel}
v_W	"	velocity of the carriage
v_L	"	landing speed
v_E	"	horizontal component of the velocity of penetration
v_{rel}	"	relative air velocity
v_{abs}	"	absolute air velocity
s	m	path
t	s	time
b	m/s^2	acceleration
G	kg	flying weight
A	"	lift
W	"	drag
g	m/s^2	earth acceleration
F	m^2	wing area
c_a		lift coefficient

c_w		drag coefficient
I	$mkgs^2$	moment of inertia
M	mkg	torque
S	kg	thrust at the center of gravity
λ		model scale
ρ	kgs^2/m^4	density
γ		inclination angle of the flight path, gliding angle
ω	$1/s$	velocity of rotation
ϵ	$1/s^2$	angular acceleration
n	$1/s$	frequency
κ		correction factor
γ^x		deviation of v_{rel} with respect to horizontal
α_R		incidence fuselage axis with respect to v_{rel}
α_g		incidence fuselage axis with respect to horizontal
β_H		angle of the elevator deflection
β_Q		angle of the aileron deflection
β_{Kl}		angle of the flap deflection
l	m	length of the airplane

Translated by Mary L. Mahler
National Advisory Committee
for Aeronautics

Covered space

Ripping panel   landing space   Gate   Cleat   Guidearm   Tank   Towing carriage

2 m

0.5 m

2.5 m

5 m

Ripping panel

Row of mirrors
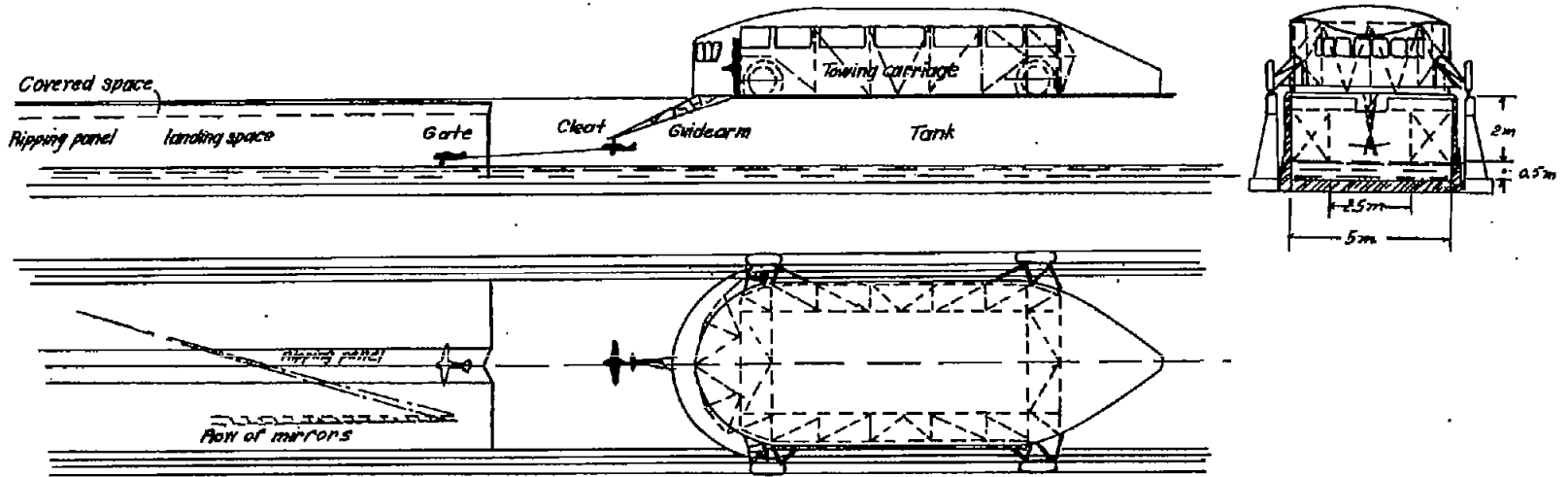
Figure 1.-   Test arrangement for investigations on landings.
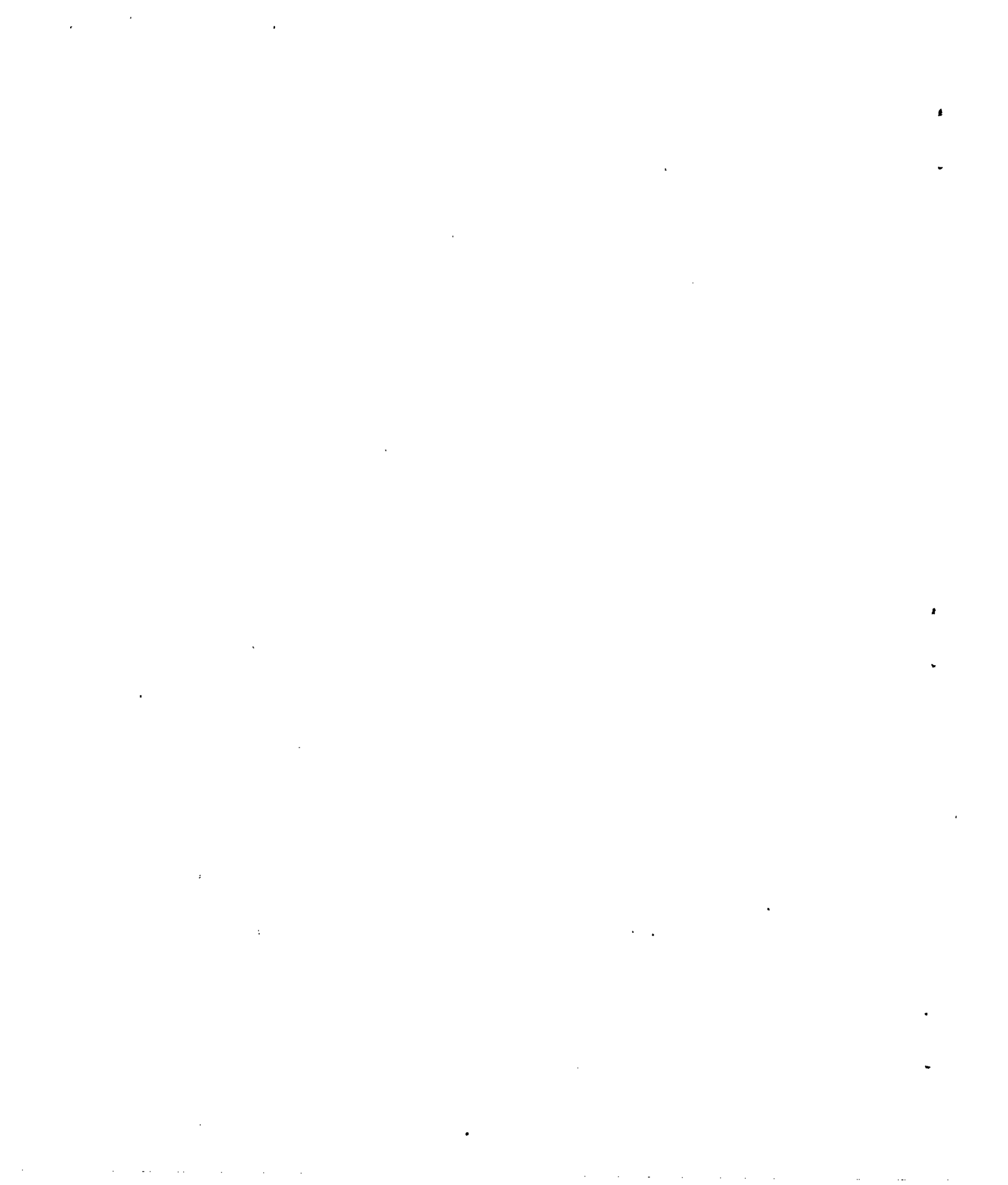
Figure 2.- Suspension of the model on the guide arm.

(This photograph was totally illigible in the only available copy of the
original German paper.)

Figure 3.- Covered space with gate.
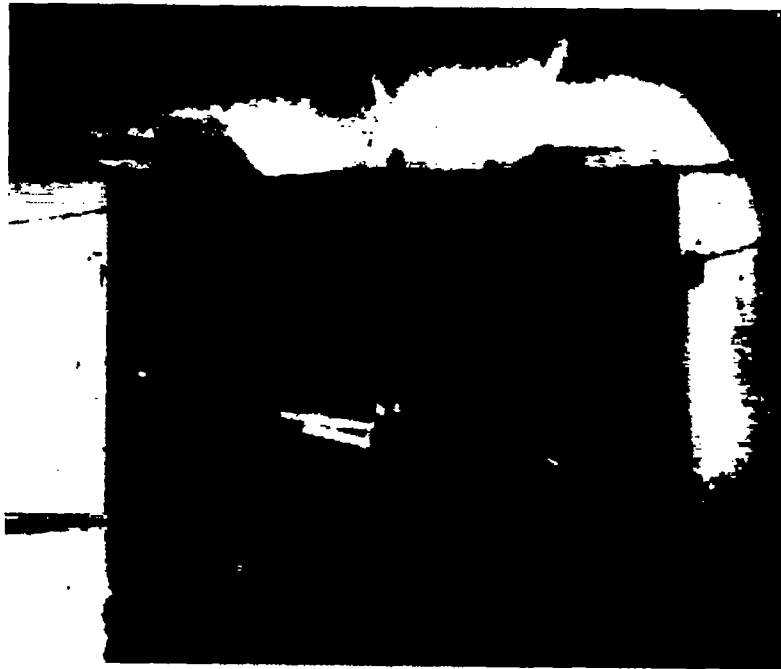
Figure 4.- Model being towed in.
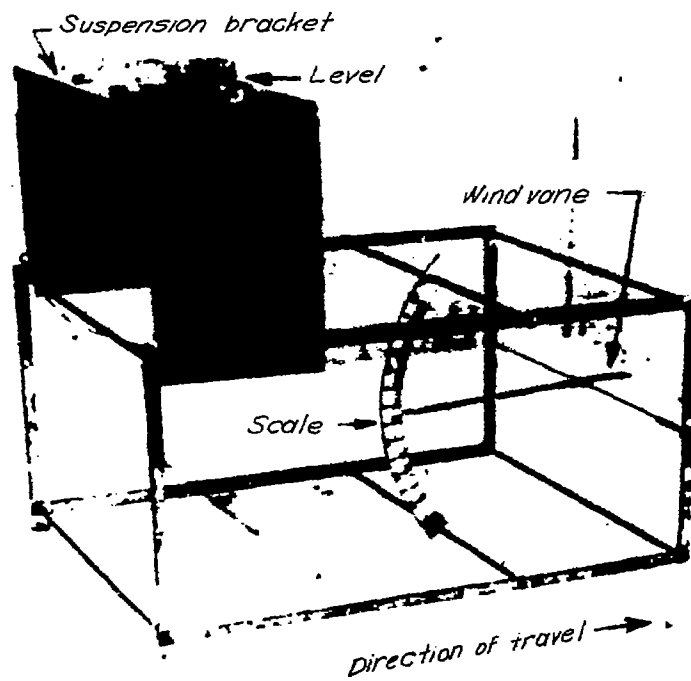
Figure 5.- Wind vane.
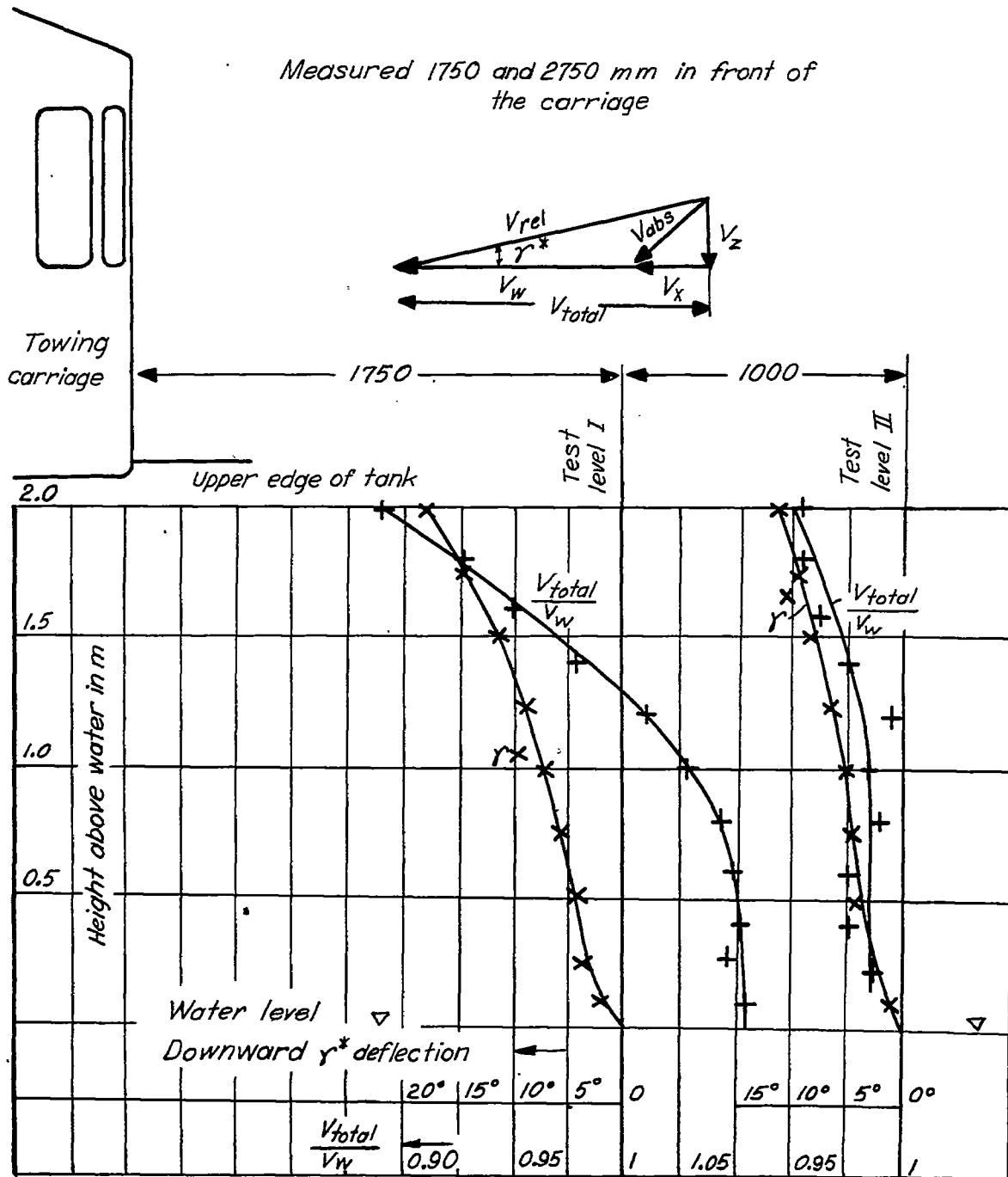
Figure 6.- Velocity and flow direction of the air in front of the towing
carriage at center of tank.

(a) Starting flight on guide arm

$$\alpha_R = \alpha g - \gamma^x$$

(b) Gliding flight

$$\alpha_R = \alpha g + \gamma$$
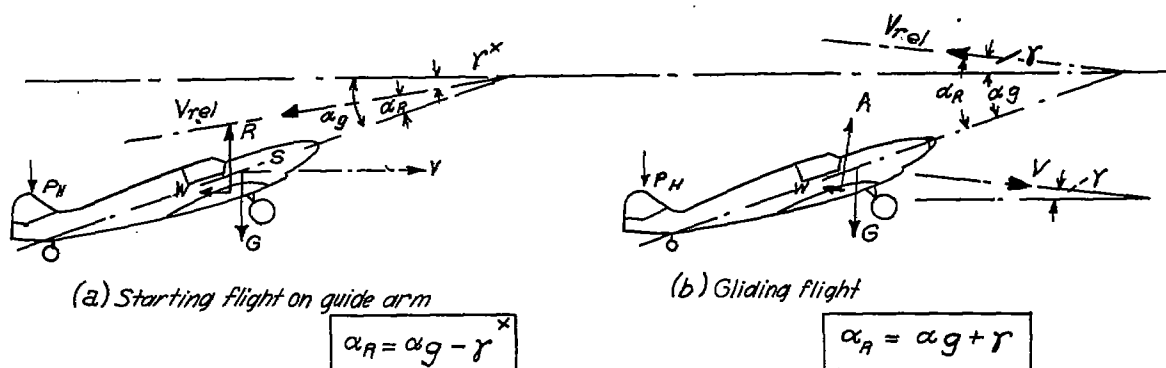
Figure 7.- Forces on the model at the guide arm in gliding flight.

$l = 1.08$

0.015

$b = 1.25$

$h = 0.3$

0.3

Model scale 1:8
Span $b = 1.25\,m$
Length $l = 1.08\,m$
Height $h = 0.3\,m$
Flying weight $G = 3.71\,kg$
Moment of inertia $I_y = 0.021\,m\,kg\,s^2$
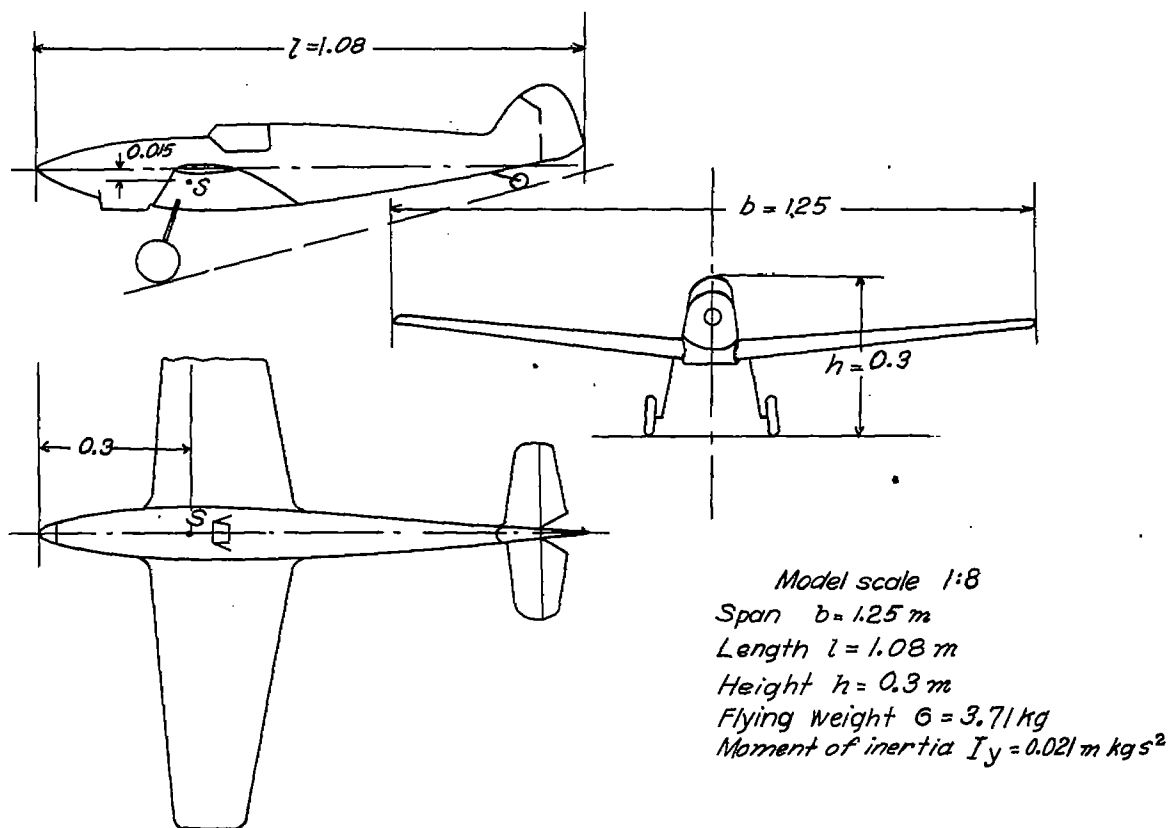
Figure 8.- Model sketch Bf 109.

Figure 9.- Model of the BF 109.
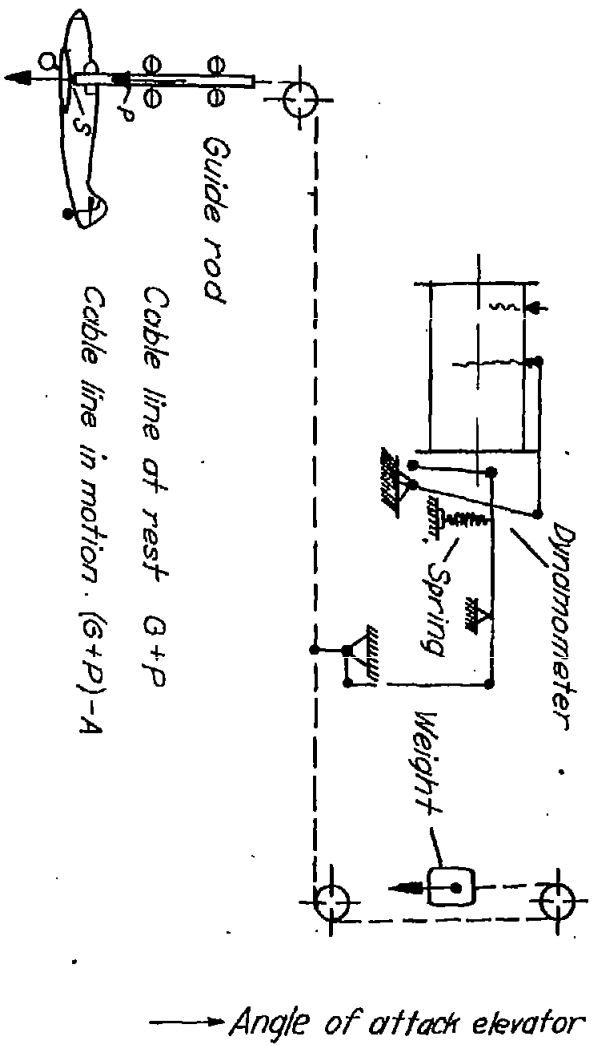
Figure 10.- Scheme of the lift measurement.
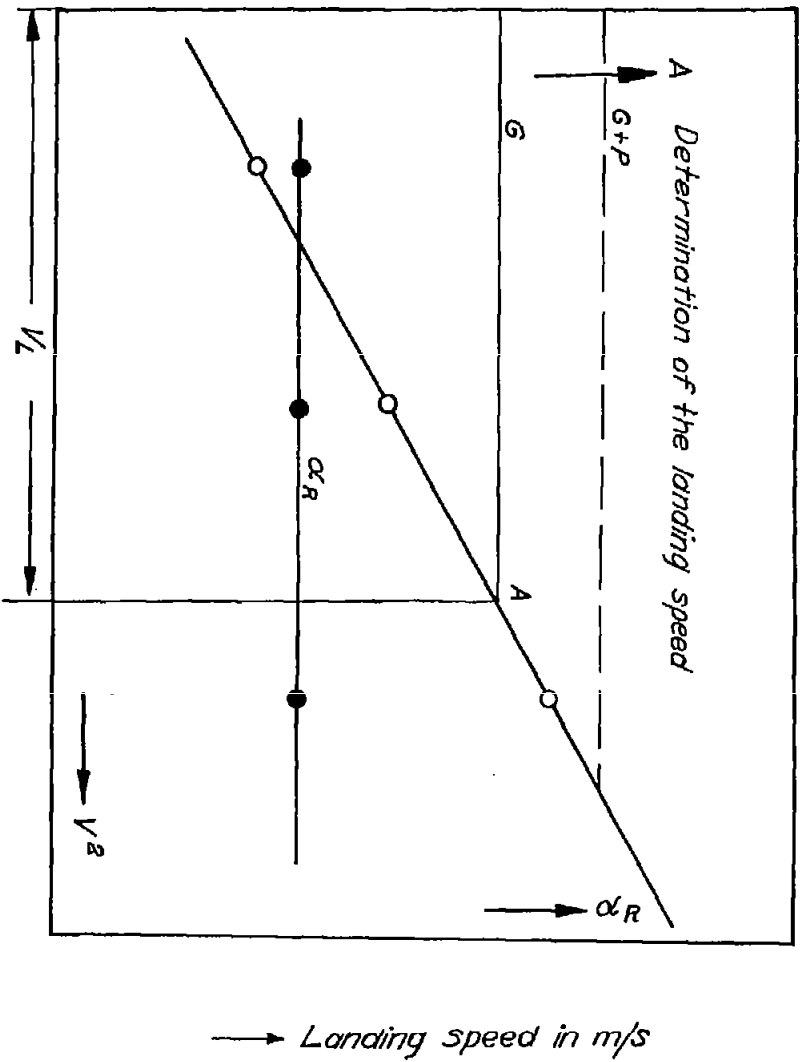
Figure 11.- Scheme for determination of the landing speed.
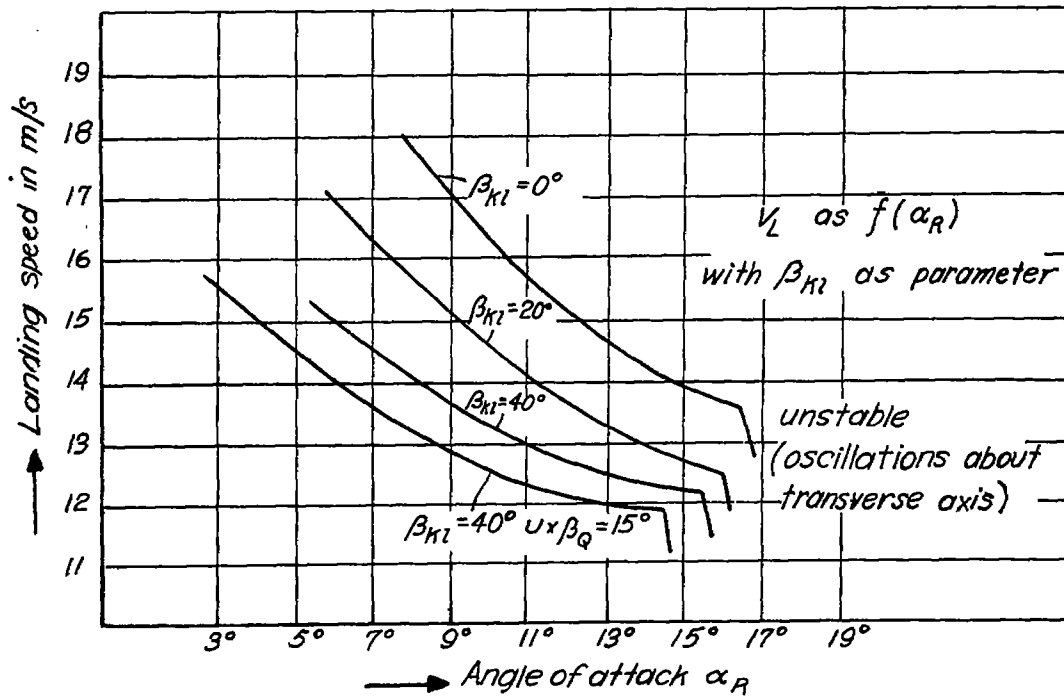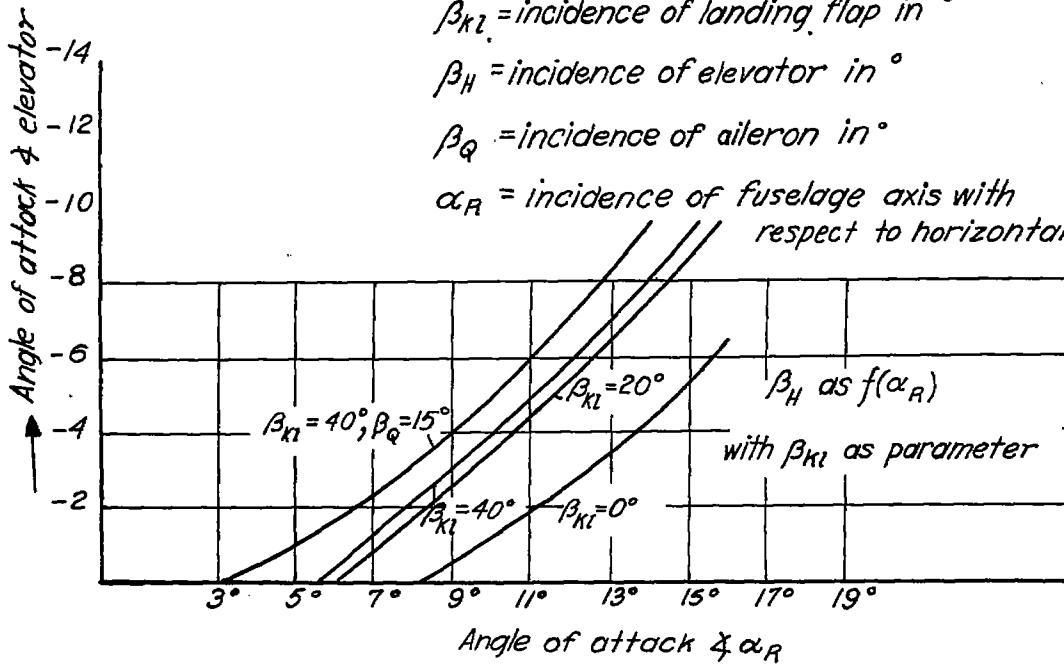
Figure 12.- Landing speeds of the model Bf 109.
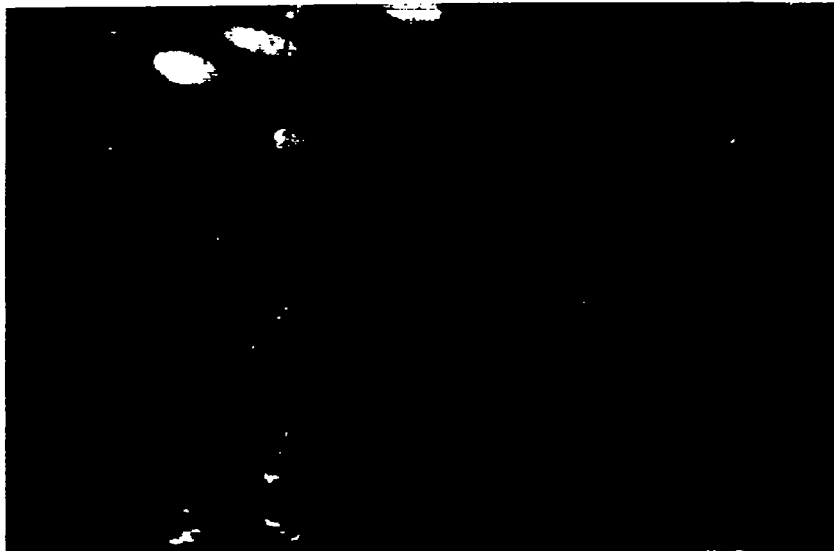
Figure 13.- Landing model with row of mirrors.
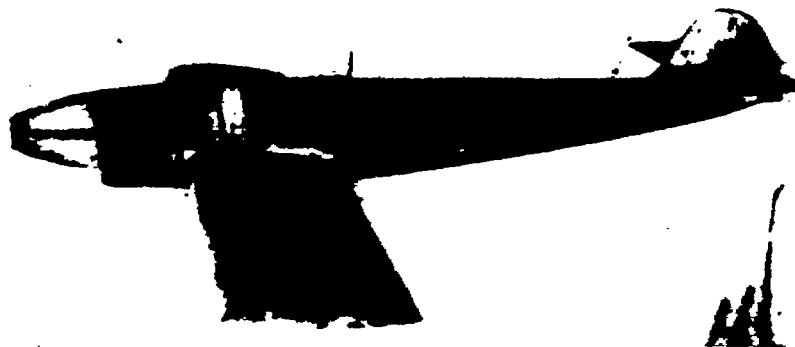
Figure 14.- Trial model.

Figure 15.- Model BF 109 without radiator.
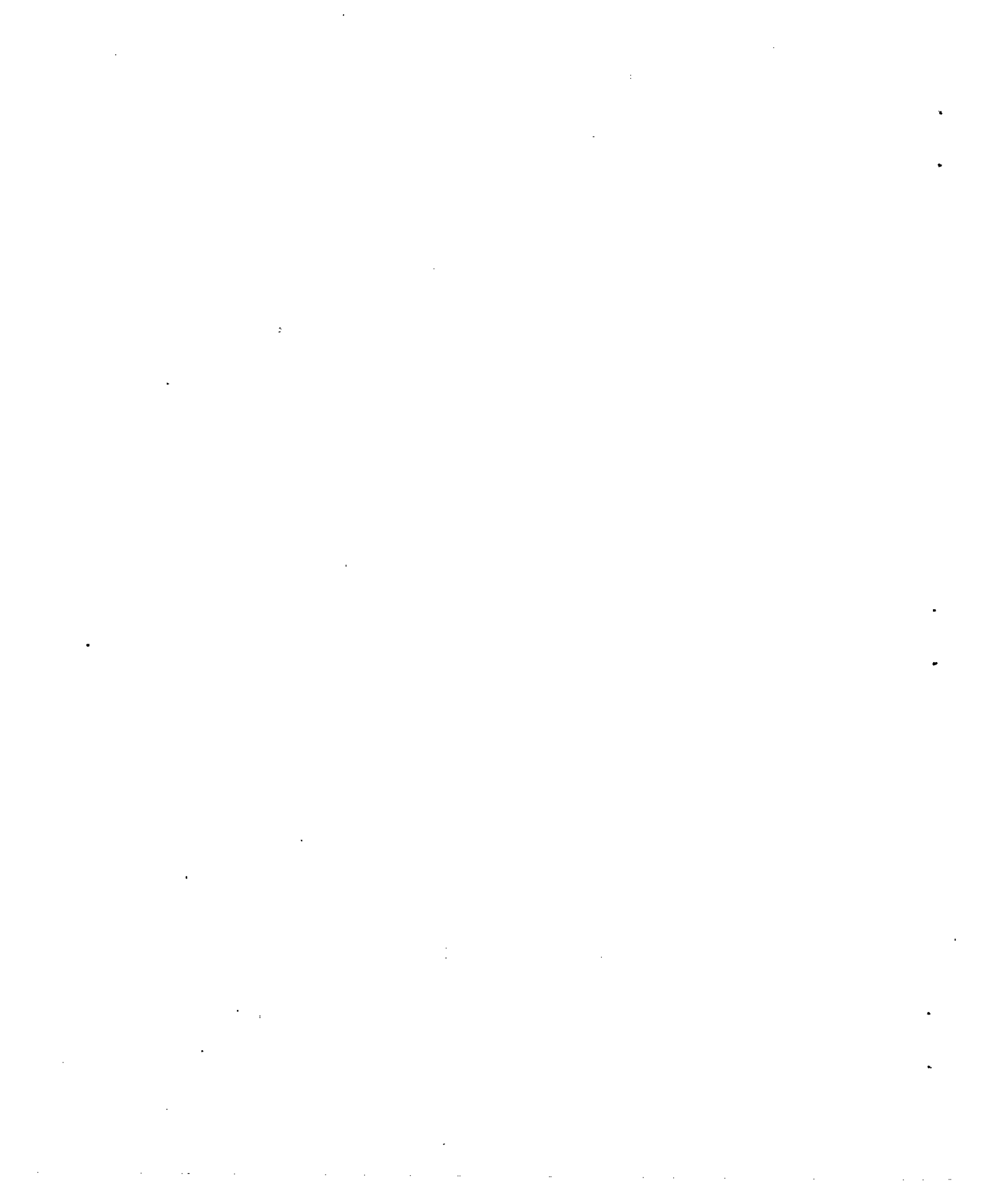
Figure 16.-   Model BF 109 with cowled radiator.

Figure 17.-   Model BF 109 with short brake hook.

Radiator covering

Fuselage

Radiator

Scale 1:1

Brake skid

Design for landing test

X With short skid toward a

XI With lengthened skid toward b

XII With lengthened skid toward b
and enlarged braking surface c

a

b

c
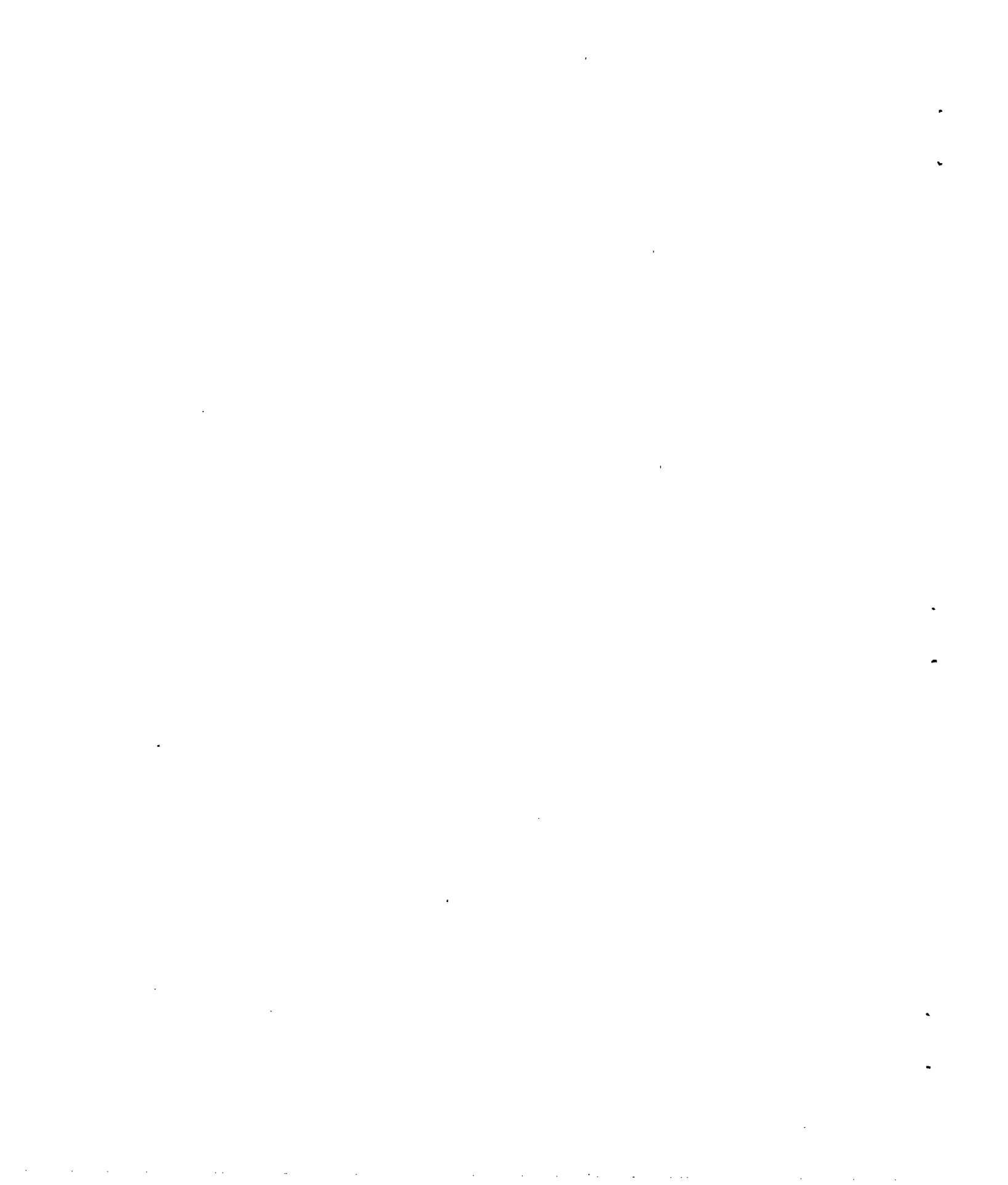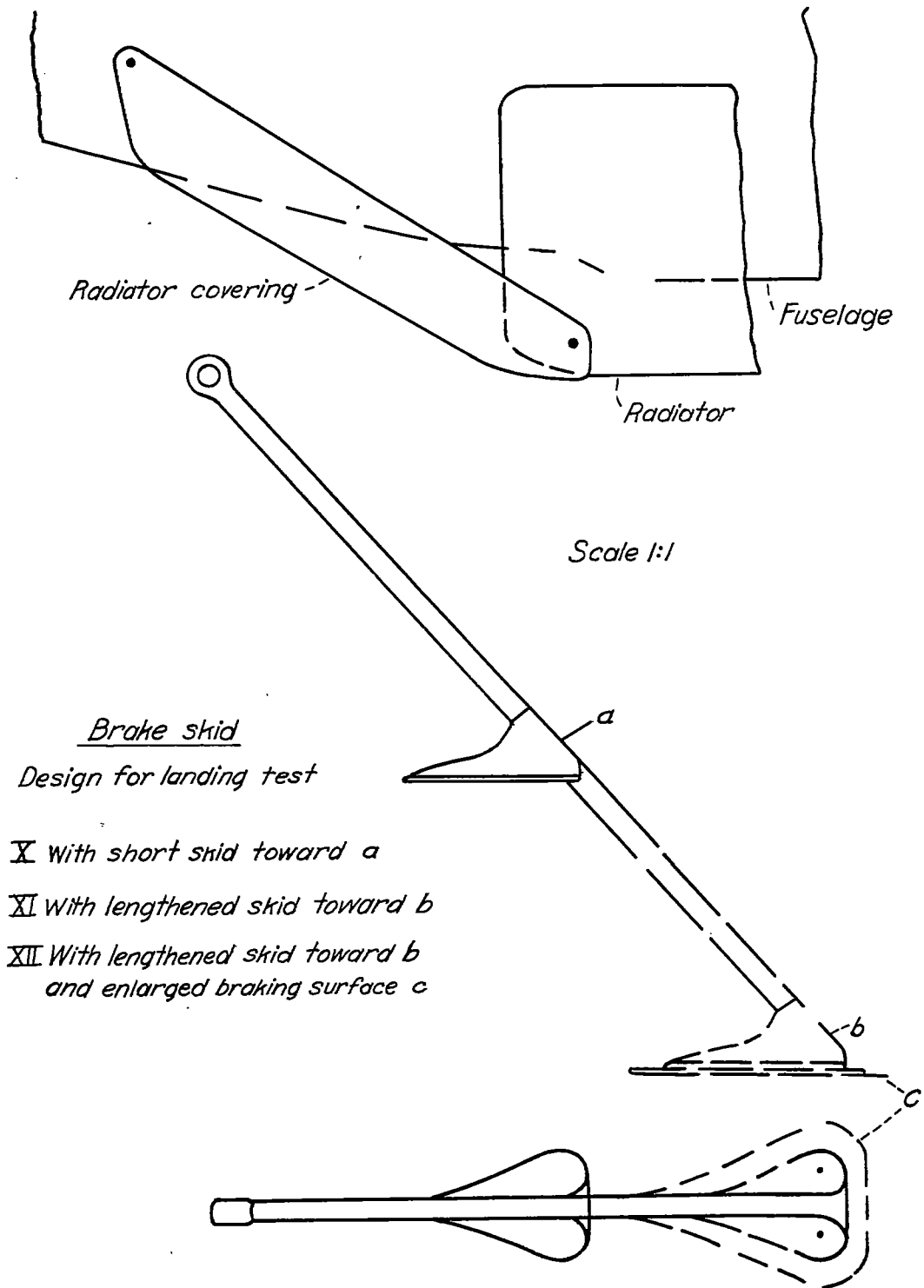
Figure 18.- Scale sketch of brake hook and radiator cowling.
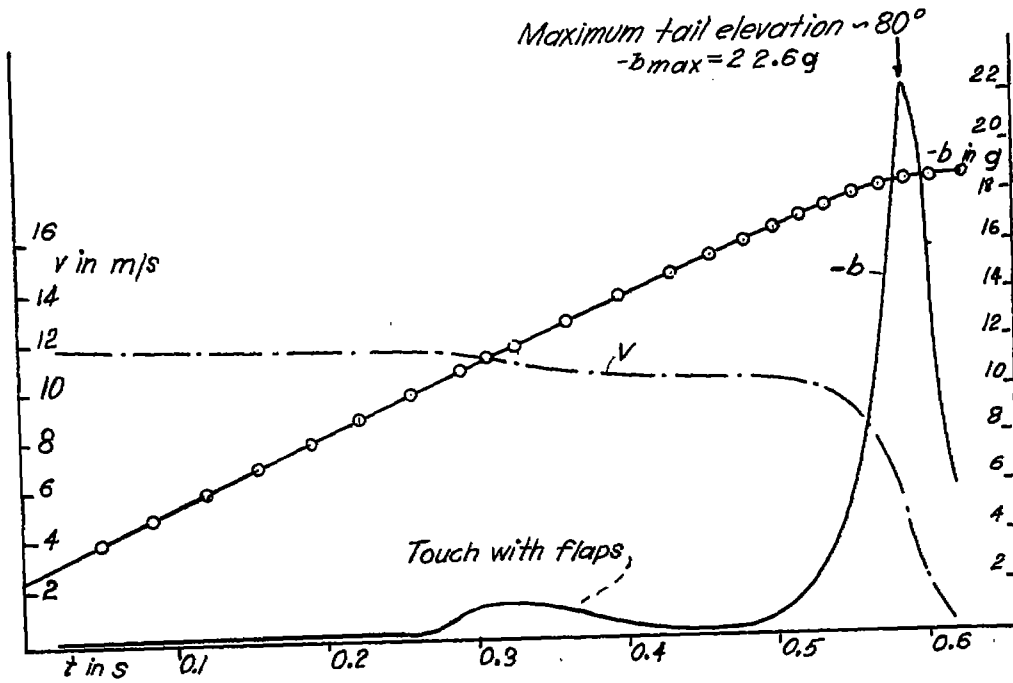
Figure 19.- Result landing test V.
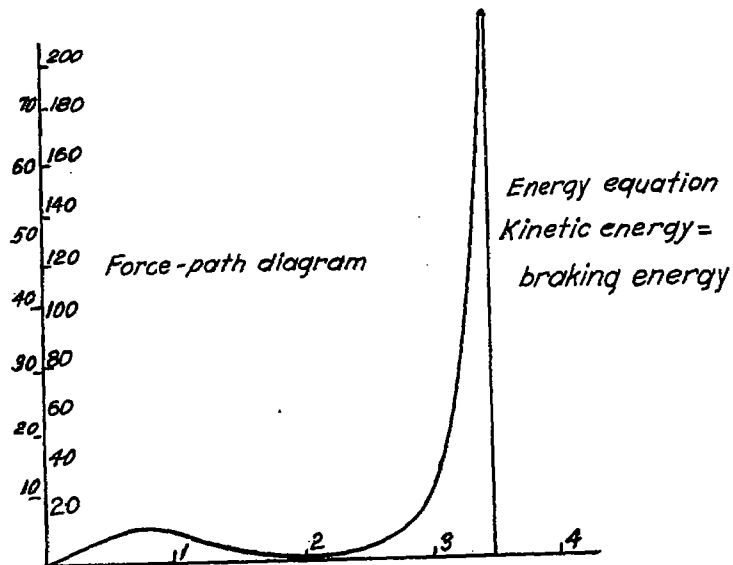
Figure 19(a).- Energy consideration for control of differentiation, landing V.
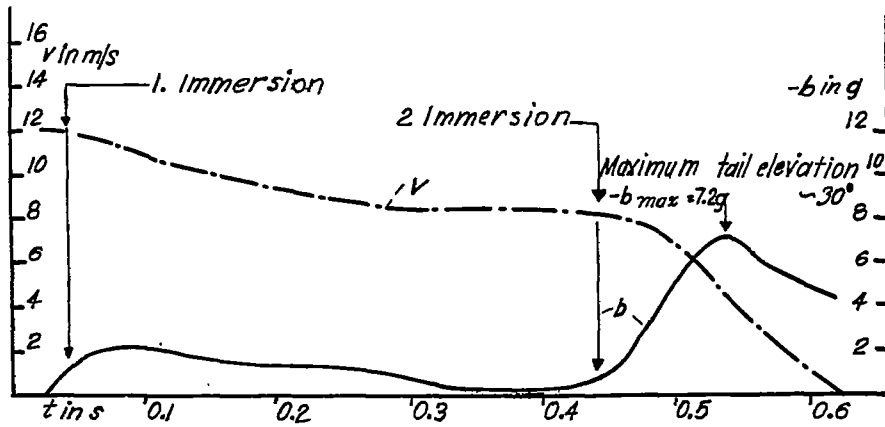
Figure 20.- Result landing test VIII.
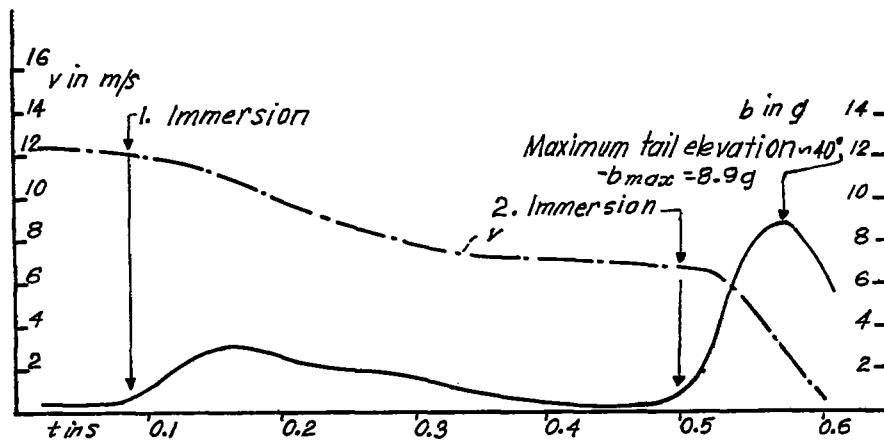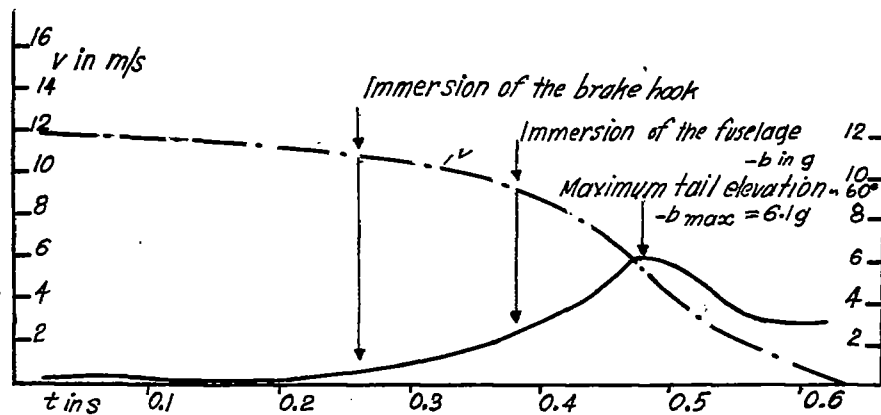

Figure 21.- Result landing test IX.
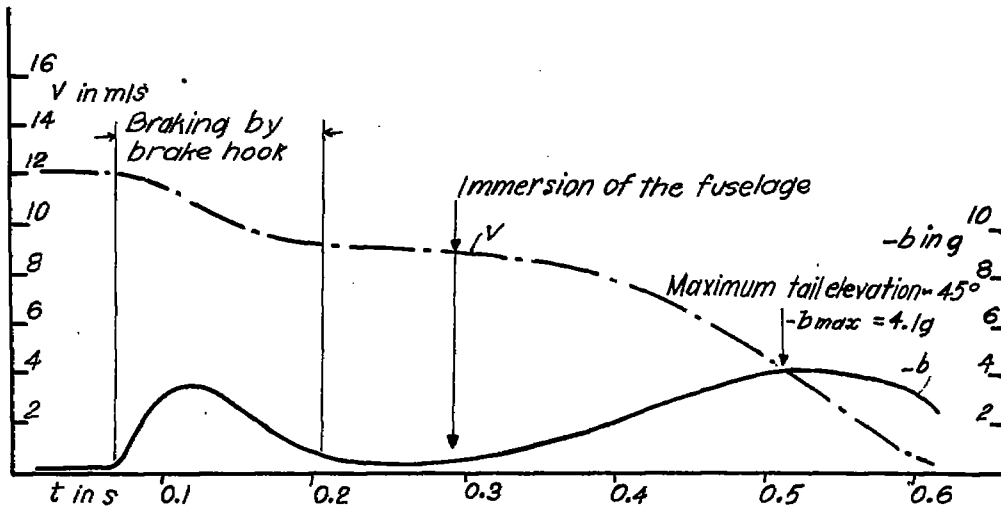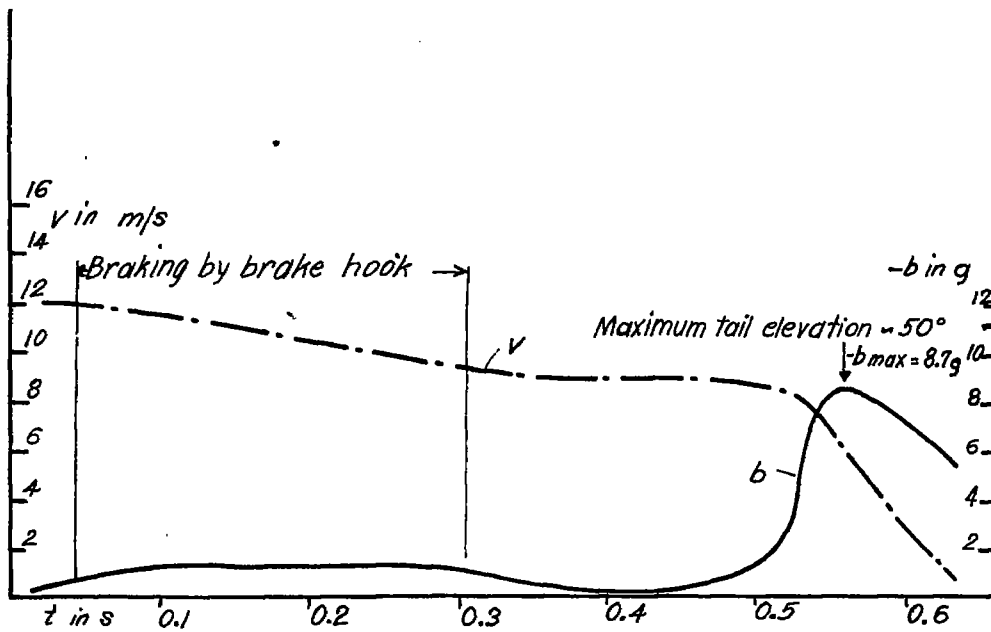

Figure 22.- Result landing test X.

Figure 23.- Result landing test XI.

Figure 24.- Result landing test XII.